GEOPHYSICS, VOL. 57, NO. 11 (NOVEMBER 1992); P. 1396–1408, 17 FIGS., 1 TABLE.

Seismic properties of pore fluids

Michael Batzle* and Zhijing Wang‡

ABSTRACT

Pore fluids strongly influence the seismic properties of rocks. The densities, bulk moduli, velocities, and viscosities of common pore fluids are usually oversimplified in geophysics. We use a combination of thermodynamic relationships, empirical trends, and new and published data to examine the effects of pressure, temperature, and composition on these important seismic properties of hydrocarbon gases and oils and of brines. Estimates of in-situ conditions and pore fluid composition yield more accurate values of these fluid properties than are typically assumed. Simplified expressions are developed to facilitate the use of realistic fluid properties in rock models.

Pore fluids have properties that vary substantially, but systematically, with composition, pressure, and temperature. Gas and oil density and modulus, as well as oil viscosity, increase with molecular weight and pressure, and decrease with temperature. Gas viscosity has a similar behavior, except at higher temperatures and lower pressures, where the viscosity will increase slightly with increasing temperature. Large amounts of gas can go into solution in lighter oils and substantially lower the modulus and viscosity. Brine modulus, density, and viscosities increase with increasing salt content and pressure. Brine is peculiar because the modulus reaches a maximum at a temperature from 40 to 80°C. Far less gas can be absorbed by brines than by light oils. As a result, gas in solution in oils can drive their modulus so far below that of brines that seismic reflection bright spots may develop from the interface between oil saturated and brine saturated rocks.

INTRODUCTION

Primary among the goals of seismic exploration are the identification of the pore fluids at depth and the mapping of hydrocarbon deposits. However, the seismic properties of these fluids have not been extensively studied. The fluids within sedimentary rocks can vary widely in composition and physical properties. Seismic interpretation is usually based on very simplistic estimates of these fluid properties and, in turn, on the effects they impart to the rocks. Pore fluids form a dynamic system in which both composition and physical phases change with pressure and temperature. Under completely normal in-situ conditions, the fluid properties can differ so substantially from the expected values that expensive interpretive errors can be made. In particular, the drastic changes possible in oils indicate that oils can be differentiated from brines seismically and may even produce reflection bright spots (Hwang and Lellis, 1988; Clark, 1992).

We will examine properties of the three primary types of pore fluids: hydrocarbon gases, hydrocarbon liquids (oils) and brines. Hydrocarbon composition depends on source, burial depth, migration, biodegradation, and production history. The schematic diagram in Figure 1 of hydrocarbon generation with depth shows that we can expect a variety of oils and gases as we drill at a single location. Hydrocarbons form a continuum of light to heavy compounds ranging from almost ideal gases to solid organic residues. At elevated pressures, the properties of gases and oils merge and the distinction between the gas and liquid phases becomes meaningless. Brines can range from nearly pure water to saline solutions of nearly 50 percent salt. In addition, oil and brine properties can be dramatically altered if significant amounts of gas are absorbed. Finally, we must be concerned with multiphase mixtures since reservoirs usually have substantial brine saturations.

Manuscript received by the Editor August 3, 1990; revised manuscript received March 3, 1992.
*ARCO Exploration and Production Technology, 2300 W. Plano Parkway, Plano, TX 75075.
‡Formerly CORE Laboratories, Calgary, Alberta T2E 2R2, Canada; presently Chevron Oil Field Research Co., 1300 Beach Blvd., La Habra, CA 90633.

Numerous mathematical models have been developed that describe the effects of pore fluids on rock density and seismic velocity (e.g., Gassmann, 1951; Biot, 1956a, b and 1962; Kuster and Toksöz, 1974; O'Connell and Budiansky, 1974; Mavko and Jizba, 1991). In these models, the fluid density and bulk modulus are the explicit fluid parameters used. In addition, fluid viscosity has been shown to have a substantial effect on rock attenuation and velocity dispersion (e.g., Biot, 1956a, b and 1962; Nur and Simmons, 1969; O'Connell and Budiansky, 1977; Tittmann et al., 1984; Jones, 1986; Vo-Thanh, 1990). Therefore, we present density, bulk modulus, and viscosity for each fluid type. Many rock models have been applied directly in oil exploration, and expressions to calculate fluid properties can allow these more realistic fluid characteristics to be incorporated.

The densities, moduli (or velocities), and viscosities of typical pore fluids can be calculated easily if simple estimates of fluid type and composition can be made. We present simplified relationships for these properties valid under most exploration conditions, but must omit most of the mathematical details. The most immediate applications of these properties will be in bright spot evaluation, amplitude versus offset analysis (AVO), log interpretation, and wave propagation models. We will not examine the role of fluid properties on seismic interpretation; neither will we explicitly calculate the effects of fluids on bulk rock properties, since this topic was covered previously (Wang et al., 1990). Nor will we consider other pore fluids that are occasionally encountered (nitrogen, carbon dioxide, drilling fluids, etc.) Even though our analyses can be further complicated by rock-fluid interactions and by the characteristics of the rock matrix, the gas, oil, and brine properties presented here should be adequate for many seismic exploration applications.

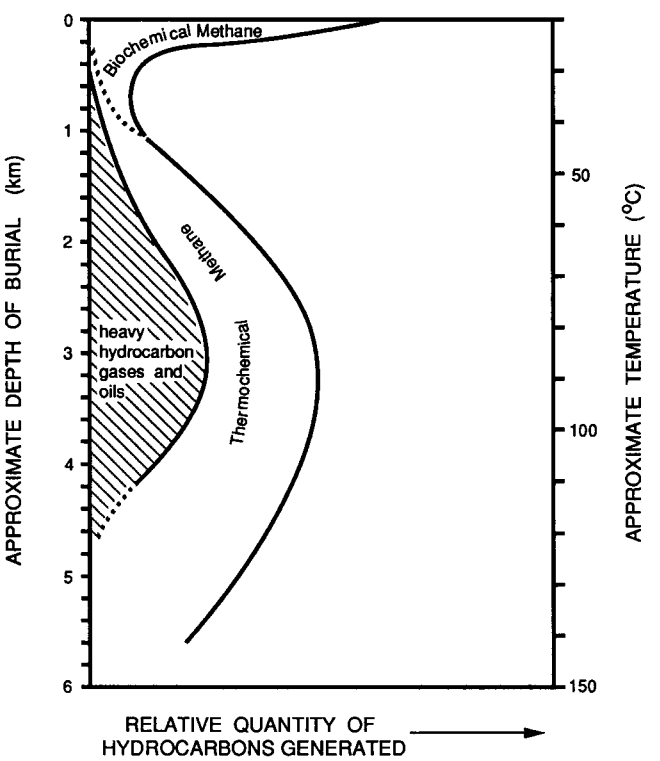

FIG. 1. A schematic of the relation of liquid and gaseous hydrocarbons generated with depth of burial and temperature (modified from Hedberg, 1974; and Sokolov, 1968). A geothermal gradient of 0.0217°C/m is assumed.

GAS

The gas phase is the easiest to characterize. The compounds are relatively simple and the thermodynamic properties have been examined thoroughly. Hydrocarbon gases usually consist of light alkanes (methane, ethane, propane, etc.). Additional gases, such as water vapor and heavier hydrocarbons, will occur in the gas depending on the pressure, temperature, and history of the deposit. Gas mixtures are characterized by a specific gravity, G, the ratio of the gas density to air density at 15.6°C and atmospheric pressure. Typical gases have G values from 0.56 for nearly pure methane to greater than 1.8 for gases with heavier components of higher carbon number. Fortunately, when only a rough idea of the gas gravity is known, a good estimate can be made of the gas properties at a specified pressure and temperature.

The important seismic characteristics of a fluid (the bulk modulus or compressibility, density, and sonic velocity) are related to primary thermodynamic properties. Hence, for gases, we naturally start with the ideal gas law:

$$\bar{V} = \frac{RT_a}{P}, \tag{1}$$

where P is pressure, $\bar{V}$ is the molar volume, R is the gas constant, and T_a is the absolute temperature [$T_a = T$ (°C) + 273.15]. This equation leads to a density ρ of

$$\rho = \frac{M}{\bar{V}} = \frac{MP}{RT_a}, \tag{2}$$

where M is the molecular weight. The isothermal compressibility β_T is

$$\beta_T = \frac{-1}{\bar{V}}\left(\frac{\partial \bar{V}}{\partial P}\right)_T, \tag{3}$$

where the subscript T indicates isothermal conditions.

If we calculate the isothermal compressional wave velocity V_T we find

$$V_T^2 = \frac{1}{\beta_T \rho} = \frac{RT_a}{M}. \tag{4}$$

Hence, for an ideal gas, velocity increases with temperature and is independent of pressure.

To bring this ideal relationship closer to reality, two mitigating factors must be considered. First, since an acoustic wave passes rapidly through a fluid, the process is adiabatic not isothermal. In most solid materials, the difference between the isothermal and adiabatic compressibilities is negligible. However, because of the larger coefficient of thermal expansion in fluids, the temperature changes associated with the compression and dilatation of an acoustic wave have a substantial effect. Adiabatic compressibility is related to isothermal compressibility through γ, the ratio of

heat capacity at constant pressure to heat capacity at constant volume; i.e.,

$$\gamma\beta_S = \beta_T. \tag{5}$$

Under reasonable exploration pressure and temperature conditions, the isothermal value can differ from the adiabatic by more than a factor of two (Johnson, 1972).

The heat capacity ratio (difficult to measure directly) can be written in terms of the more commonly measured constant pressure heat capacity (C_P), thermal expansion (α), isothermal compressibility, and volume (Castellan, 1971, p. 219)

$$\frac{1}{\gamma} = 1 - \frac{T_a \bar{V} \alpha^2}{C_P \beta_T}. \tag{6}$$

These properties, in turn, can be derived from an equation of state of the fluid and a reference curve of C_P at some given pressure.

The second and more obvious correction stems from the inadequacies of the ideal gas law [equation (1)]. A more realistic description includes the compressibility factor Z;

$$\bar{V} = \frac{ZRT_a}{P}. \tag{7}$$

Following the same procedure as in equations (3) to (5), we get the relationship for adiabatic bulk modulus K_S,

$$K_S = \frac{1}{\beta_S} = \frac{\gamma P}{\left(1 - \frac{P}{Z}\frac{\partial Z}{\partial P}\right)_T}. \tag{8}$$

The modulus can be obtained, therefore, if Z can be adequately described.

The variable composition of natural gases adds a further complication in any attempt to describe their properties. For pure compounds, the gas and liquid phases exist in equilibrium along a specific pressure-temperature curve. As pressure and temperature are increased, the properties of the two phases approach each other until they merge at the critical point. For mixtures, this point of phase homogenization depends on the composition and is referred to as the pseudocritical point with pseudocritical temperature T_{pc} and pressure P_{pc}. The properties of mixtures can be made more systematic when temperatures and pressures are normalized or "pseudoreduced" by the pseudocritical values (Katz et al., 1959). Thomas et al., (1970) examined numerous natural gases and found simple relationships between G and the pseudoreduced pressure P_{pr} and pseudoreduced temperature T_{pr}.

$$P_{pr} = P/P_{pc} = P/(4.892 - 0.4048\ G), \tag{9a}$$

$$T_{pr} = T_a/T_{pc} = T_a/(94.72 + 170.75\ G), \tag{9b}$$

where P is in MPa. They then used these pseudoreduced pressures and temperatures in the Benedict-Webb-Rubin (BWR) equation of state to calculate velocities. The BWR equation is a complex algebraic expression that can be solved iteratively for molar volume and thus modulus and density. Younglove and Ely (1987) developed more precise BWR equations and tabulated both densities and velocities, but only for pure compounds. The approach using pseudoreduced values is preferable for mixtures, and components such as CO_2 and N_2 can even be incorporated by using molar averaged T_{pc} and P_{pc}.

Gas densities derived from the Thomas et al., (1970) relations are shown in Figure 2. Alternatively, for the pressures and temperatures typically encountered in oil exploration, we can use the approximation

$$\rho \cong \frac{28.8GP}{ZRT_a}, \tag{10a}$$

where

$$Z = [0.03 + 0.00527(3.5 - T_{pr})^3]P_{pr} + (0.642T_{pr} - 0.007T_{pr}^4 - 0.52) + E \tag{10b}$$

and

$$E = 0.109(3.85 - T_{pr})^2 \exp\{-[0.45 + 8(0.56 - 1/T_{pr})^2]P_{pr}^{1.2}/T_{pr}\}. \tag{10c}$$

This approximation is adequate as long as P_{pr} and T_{pr} are not both within about 0.1 of unity. As expected, the gas densities increase with pressure and decrease with temperature. However, Figure 2 also demonstrates how the densities are strongly dependent on the composition of the gas mixture.

The adiabatic gas modulus K_S is also strongly dependent on composition. Figure 3 shows the modulus derived from Thomas et al., (1970). As with the density, the modulus increases with pressure and decreases with temperature. The impact of composition is particularly dynamic at low temperatures. Again, a simpler form can be used to approximate K_S under typical exploration conditions, but with the same restriction as for equation (10).

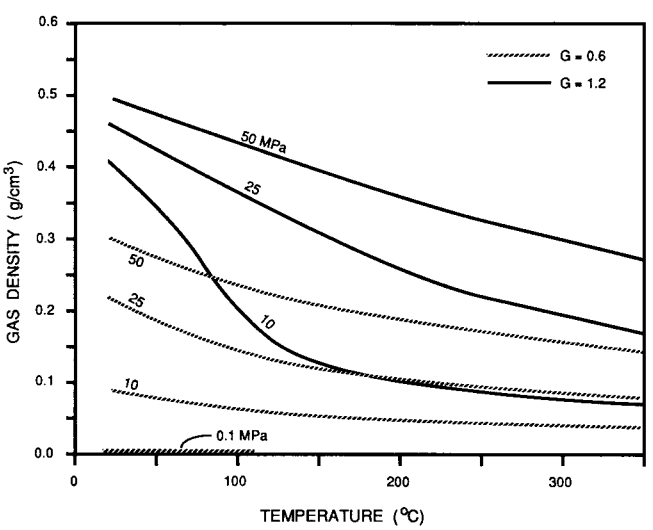

FIG. 2. Hydrocarbon gas densities as a function of temperature, pressure, and composition. Densities are plotted for a light gas ($\rho_{gas}/\rho_{air} = G = 0.6$ at 15.5°C and 0.1 MPa). and heavy gas ($G = 1.2$). Values for light and heavy gases overlay at 0.1 MPa.

$$K_S \cong \frac{P}{\left(1 - \frac{P_{pr}}{Z}\frac{\partial Z}{\partial P_{pr}}\right)_T}\gamma_0, \qquad (11a)$$

where

$$\gamma_0 = 0.85 + \frac{5.6}{(P_{pr} + 2)} + \frac{27.1}{(P_{pr} + 3.5)^2} - 8.7 \exp[-0.65(P_{pr} + 1)]. \qquad (11b)$$

Values for $\partial Z/\partial P_{pr}$ are easily obtained from equations (10b) and (10c).

The velocities calculated by Thomas et al., (1970) from the equation of state show several percent error when compared to direct measurements of velocity in methane (Gammon and Douslin, 1976) or the tabulated values of Younglove and Ely (1987). Small errors in the volume calculations of the BWR equation transform into much larger errors in the calculated velocity. In spite of this, the Thomas et al., (1970) relationships have the advantage of applicability to a wide range in hydrocarbon gas composition.

To complete our description of gas properties, we need to examine viscosity. The viscosity of a simple, single component gas can be calculated using the kinetic theory of molecular motion. This procedure would be similar to our derivation of modulus from the ideal gas law. When the compositions become complex however, more empirical methods must be used. Petroleum engineers have made extensive studies of gas viscosity because of its importance in fluid transport problems (see, for example, Carr et al., 1954; Katz et al., 1959). We will include some simple relationships here although more precise calculations can be made, particularly if there is detailed information on the gas composition.

The viscosity of an ideal gas is controlled by the momentum transfer provided by molecular movement between regions of shear motion. Such a kinetic theory predicts almost no pressure dependence for viscosity, but rather an increase in viscosity with increasing temperature. This behavior is in contrast to most other fluids. At atmospheric pressure, gas viscosity can be described by

$$\eta_1 = 0.0001[T_{pr}(28 + 48\ G - 5G^2) - 6.47\ G^{-2} + 35\ G^{-1} + 1.14\ G - 15.55], \qquad (12)$$

where η_1 is in centipoise. The viscosity of gas at pressure η is then related to the low pressure viscosity by

$$\eta/\eta_1 = 0.001P_{pr}\left[\frac{1057 - 8.08T_{pr}}{P_{pr}} + \frac{796\ P_{pr}^{1/2} - 704}{(T_{pr} - 1)^{0.7}(P_{pr} + 1)} - 3.24T_{pr} - 38\right]. \qquad (13)$$

Figure 4 shows the calculated viscosities for light ($G = 0.6$) and heavy ($G = 1.2$) gases under exploration conditions. The rapid increase in viscosity of the heavy gas at low temperature is indicative of approaching the pseudocritical point. As with many of the other physical properties, if gas from a specific location is very well characterized, the viscosity usually can be more accurately calculated by our associates in petroleum engineering.

OIL

Crude oils can be mixtures of extremely complex organic compounds. Natural oils range from light liquids of low carbon number to very heavy tars. At the heavy extreme are bitumen and kerogen which may be denser than water and act essentially as solids. At the light extreme are condensates which have become liquid as a result of the changing pressures and temperatures during production. In addition, light oils under pressure can absorb large quantities of hydrocarbon gases, which significantly decrease the moduli and density. Under room conditions, oil densities can vary from under 0.5 g/cm^3 to greater than 1 g/cm^3, with most produced oils in the 0.7 to 0.8 g/cm^3 range. A reference density that can be used to characterize an oil ρ_0 is measured

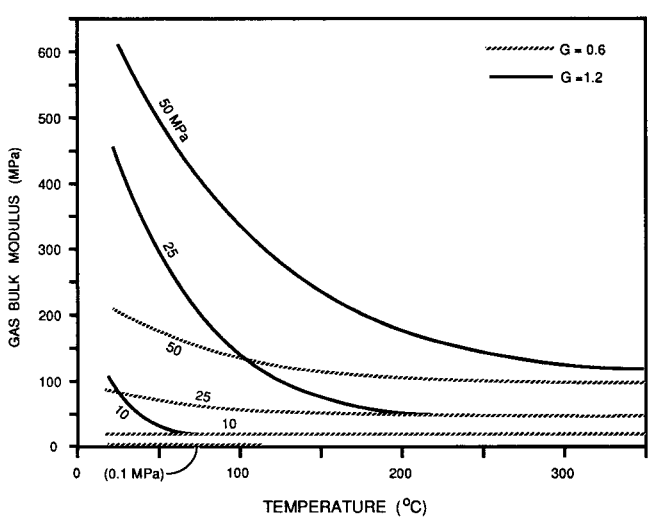

FIG. 3. The bulk modulus of hydrocarbon gas as a function of temperature, pressure, and composition. As in Figure 2, the values for the light and heavy gases overlay at 0.1 MPa.

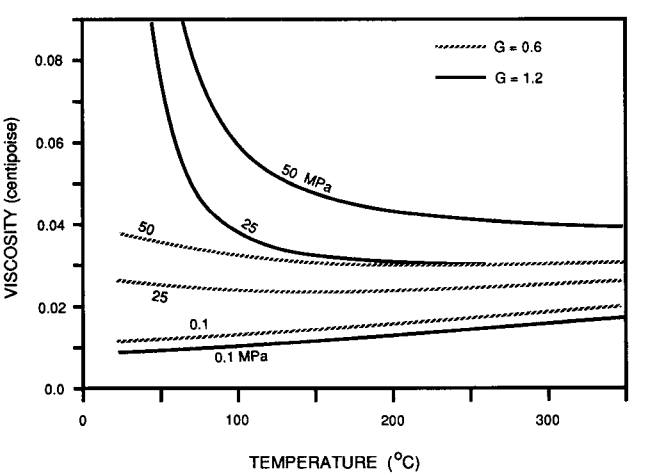

FIG. 4. Calculated viscosity of hydrocarbon gases.

at 15.6°C and atmospheric pressure. A widely used classification of crude oils is the American Petroleum Institute oil gravity (API) number and is defined as

$$\text{API} = \frac{141.5}{\rho_0} - 131.5. \tag{14}$$

This results in numbers of about five for very heavy oils to near 100 for light condensates. This API number is often the only description of an oil that is available. The variable compositions and ability to absorb gases produce wide variations in the seismic properties of oils. However, these variations are systematic and by using ρ_0 or the API gravity we can make reasonable estimates of oil properties.

If we had a general equation of state for oils, we could calculate the moduli and densities as we did for the gases. Numerous such equations are available in the petroleum engineering literature; but they are almost always strongly dependent on the exact composition of a given oil. In exploration, we normally have only a rough idea of what the oils may be like. In some reservoirs, adjacent zones will have quite distinct oil types. We will, therefore, proceed first along empirical lines based on the density of the oil.

The acoustic properties of numerous organic fluids have been studied as a function of pressure or temperature. (e.g., Rao and Rao, 1959.) Generally, away from phase boundaries, the velocities, densities, and moduli are quite linear with pressure and temperature. In organic fluids typical of crude oils, the moduli decrease with increasing temperature or decreasing pressure. Wang and Nur (1986) did an extensive study of several light alkanes, alkenes, and cycloparaffins. They found simple relationships among the density, moduli, temperature, and carbon number or molecular weight. The velocity at temperature $V(T)$ varies linearly with the change in temperature ΔT from a given reference temperature.

$$V(T) = V_0 - b\Delta T, \tag{15}$$

where V_0 is the initial velocity at the reference temperature and b is a constant for each compound of molecular weight M.

$$b = 0.306 - \frac{7.6}{M}. \tag{16}$$

Similarly, the velocities are related in molecular weight by

$$V(T, M) = V_0 - b\Delta T - a_m\left(\frac{1}{M} - \frac{1}{M_0}\right), \tag{17}$$

where $V(T, M)$ is the velocity of oil of molecular weight M at temperature T, and V_0 is the velocity of a reference oil of weight M_0 at temperature T_0. The variable a_m is a positive function of temperature and so oil velocity increases with increasing molecular weight. When compounds are mixed, velocity is a simple fractional average of the end components. This is roughly equivalent to a fractional average of the bulk moduli of the end components. Pure simple hydrocarbons, therefore, behave in a simple and predictable way.

We need to extend this analysis to include crude oils which are generally much heavier and have more complex compositions. The general density variation with pressure and temperature has been examined in detail by petroleum engineers (e.g., McCain, 1973). For an oil that remains constant in composition, the effects of pressure and temperature are largely independent. The pressure dependence is comparatively small and the published data for density at pressure ρ_P can be described by the polynomial

$$\rho_P = \rho_0 + (0.00277P - 1.71 \times 10^{-7}P^3)(\rho_0 - 1.15)^2 + 3.49 \times 10^{-4}P. \tag{18}$$

The effect of temperature is larger, and one of the most common expressions used to calculate the in-situ density was developed by Dodson and Standing (1945).

$$\rho = \rho_P/[0.972 + 3.81 \times 10^{-4}(T + 17.78)^{1.175}] \tag{19}$$

The results of these expressions are shown in Figure 5.

Wang (1988) and Wang et al., (1988) showed that the ultrasonic velocity of a variety of oils decreases rapidly with density (increasing API) as shown in Figure 6. A simplified form of the velocity relationship they developed is

$$V = 2096\left(\frac{\rho_0}{2.6 - \rho_0}\right)^{1/2} - 3.7T + 4.64P + 0.0115[4.12(1.08\rho_0^{-1} - 1)^{1/2} - 1]TP. \tag{20a}$$

Or, in terms of API

$$V = 15450(77.1 + \text{API})^{-1/2} - 3.7T + 4.64P + 0.0115(0.36\text{API}^{1/2} - 1)TP, \tag{20b}$$

where V is velocity in m/s. Using this relationship with the density from equation (19), we get the oil modulus shown in Figure 7.

As an alternative approach, we could derive the velocity and adiabatic modulus using pressure-volume-temperature relationships, such as in equations (18) and (19). Heat capacity ratios may be estimated using generalized charts. This procedure can yield fairly good estimates as shown in

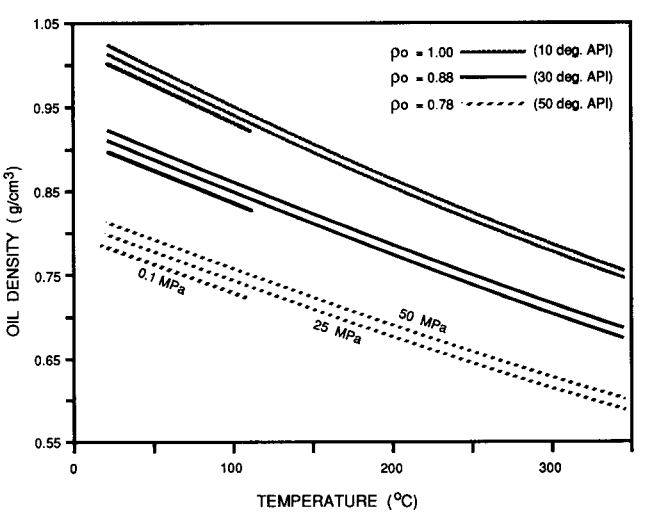

FIG. 5. Oil densities as a function of temperature, pressure, and composition.

Figure 6. However, the analysis is further complicated by the drastic changes in oil composition typical under in-situ conditions.

Large amounts of gas or light hydrocarbons can go into solution in crude oils. From the hydrocarbon generation indicated in Figure 1, large dissolved gas contents should be typical at depth. In fact, very light crude oils are often condensates from the gas phase. We would expect gas saturated oils (live oils) to have significantly different properties than the gas-free oils (dead oils) commonly measured. As an oil is produced, the original single phase fluid will separate into a gas and a liquid phase. The original fluid in-situ is usually characterized by R_G, the volume ratio of liberated gas to remaining oil at atmospheric pressure and 15.6°C. The maximum amount of gas that can be dissolved in an oil is a function of pressure, temperature, and composition of both the gas and oil.

$$R_G = 0.02123G\left[P \exp\left(\frac{4.072}{\rho_0} - 0.00377\,T\right)\right]^{1.205}, \tag{21a}$$

or, in terms of API

$$R_G = 2.03G[P \exp(0.02878\,\text{API} - 0.00377\,T)]^{1.205}, \tag{21b}$$

where R_G is in Liters/Liter (1 L/L = 5.615 cu ft/BBL) and G is the gas gravity (after Standing, 1962). Equation (21) indicates that much larger amounts of gas can go into the light (high-API number) oils. In fact, heavy oils may precipitate heavy compounds if much gas goes into solution. We have found this equation to occasionally be a more reliable indicator of in-situ gas-oil ratios than actual production records: if a reservoir is drawn down below its bubble point, gas will come out of solution and be preferentially produced.

The effect of dissolved gas on the acoustic properties of oils has not been well documented. Sergeev (1948) noted that dissolved gas reduces both oil and brine velocities. He calculated this would change some reservoir reflection coefficients by more than a factor of two. Hwang and Lellis (1988) showed the substantial decrease in moduli and densities of numerous oils with increasing gas content. They attributed several seismic bright spots to the reduced rock velocities resulting from gas-saturated oils. Similarly, Clark (1992) measured the ultrasonic velocity reduction in several oils with increasing gas content. She demonstrated how these live oils can produce dramatic responses in both seismic sections and sonic logs. Because such strong effects are possible, analyses based on dead oil properties can be grossly incorrect.

Seismic properties of a live oil are estimated by considering it to be a mixture of the original gas-free oil and a light liquid representing the gas component. Velocities can still be calculated using equation (20) by substituting a pseudodensity ρ' based on the expansion caused by gas intake.

$$\rho' = \frac{\rho_0}{B_0}(1 + 0.001R_G)^{-1}, \tag{22}$$

where B_0 is a volume factor derived by Standing (1962),

$$B_0 = 0.972 + 0.00038\left[2.4R_G\left(\frac{G}{\rho_0}\right)^{1/2} + T + 17.8\right]^{1.175}. \tag{23}$$

Figure 8 shows the live and dead oil velocities measured by Wang et al., (1988) along with calculated values using ρ'. The gas induced decreases in velocity are substantial. Below the saturation pressure (bubble point) of the live oil at about 20 MPa, free gas exsolves, and calculated velocities depart greatly from measured values.

True densities of live oils are also calculated using B_0, but the mass of dissolved gas must be included.

$$\rho_G = (\rho_0 + 0.0012GR_G)/B_0, \tag{24}$$

where ρ_G is the density at saturation. At temperatures and pressures that differ from those at saturation, ρ_G must be adjusted using equations (18) and (19). Because of this gas

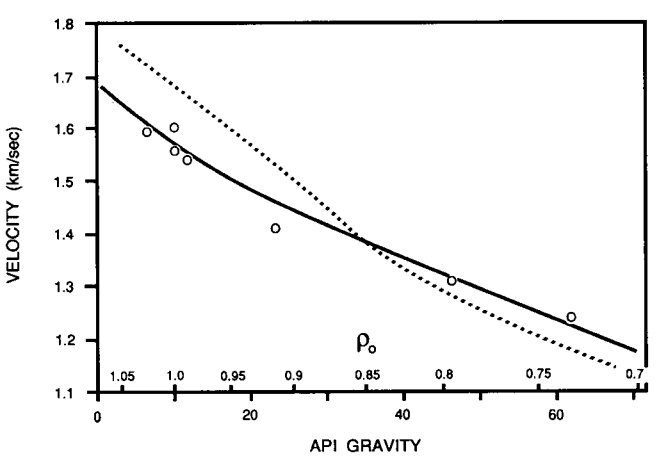

FIG. 6. Oil acoustic velocity as a function of reference density, ρ_0 (or API), using equation (20) (solid line) versus values derived from empirical phase relations (dashed line). Data (O) are at room pressure and temperature.

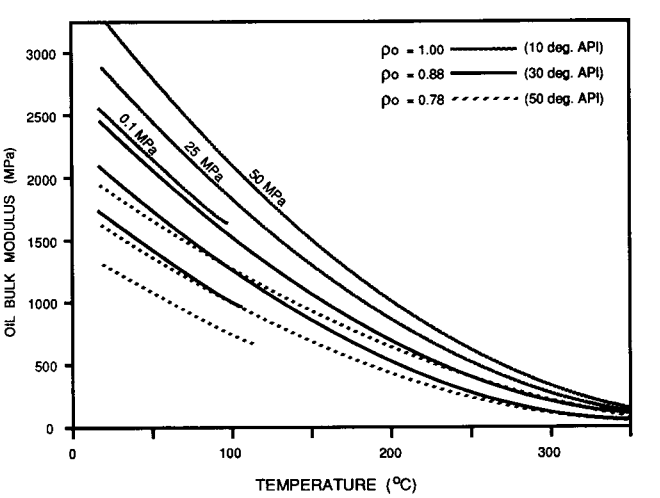

FIG. 7. The bulk modulus of oil as a function of temperature, pressure, and composition.

effect, oil densities often decrease with increasing pressure or depth as more gas goes into solution.

The viscosity of oils increases by several orders of magnitude when ρ_0 is increased (lower API) or temperature is lowered. As temperatures are lowered, oil approaches its glass point and begins to act like a solid. The velocity increases rapidly and the fluid becomes highly attenuating (Figure 9). In the seismic frequency band, this effect can be significant for tar, kerogen, or heavy organic-rich rock (e.g., Monterey formation). For logging, and particularly for laboratory ultrasonic frequencies, this effect can be a problem for produced heavy oils. Even for oils where bulk velocity is still low, the viscous skin depth can be sufficient within the confines of a small pore space to increase the rock compressional and shear velocities. This particular topic was covered in detail by Jones (1986).

Unlike gases, oil viscosity always decreases rapidly with increasing temperature since the tightly packed oil molecules gain increasing freedom of motion at elevated temperature. Beggs and Robinson (1975) provide a simple relationship for the viscosity, in centipoise, of gas-free oil as a function of temperature, η_T.

$$\mathrm{Log}_{10}(\eta_T + 1) = 0.505y(17.8 + T)^{-1.163} \quad (25a)$$

with

$$\mathrm{Log}_{10}(y) = 5.693 - 2.863/\rho_0 \quad (25b)$$

Pressure has a smaller influence, and a simple correlation was developed by Beal (1946) to obtain the corrected viscosity η at pressure.

$$\eta = \eta_T + 0.145PI, \quad (26a)$$

where

$$\mathrm{Log}_{10}(I) = 18.6[0.1\ \mathrm{Log}_{10}(\eta_T) + (\mathrm{Log}_{10}(\eta_T) + 2)^{-0.1} - 0.985]. \quad (26b)$$

The results of this relationship are plotted in Figure 10.

Gas in solution also decreases viscosity. In a typical engineering procedure, viscosity at saturation, or bubble point temperature and pressure, is calculated first then adjustments are made for pressures above saturation. Alternatively, a simple estimate can be made by using live oil density. First, B_0 is calculated for standard conditions (0.1 MPa, 15.6°C). Then the resulting value found for ρ_G is used in equations (25) and (26) in place of ρ_0. Such estimates are usually adequate for general exploration purposes, but the more precise engineering procedures should be used if the exact oil composition is known.

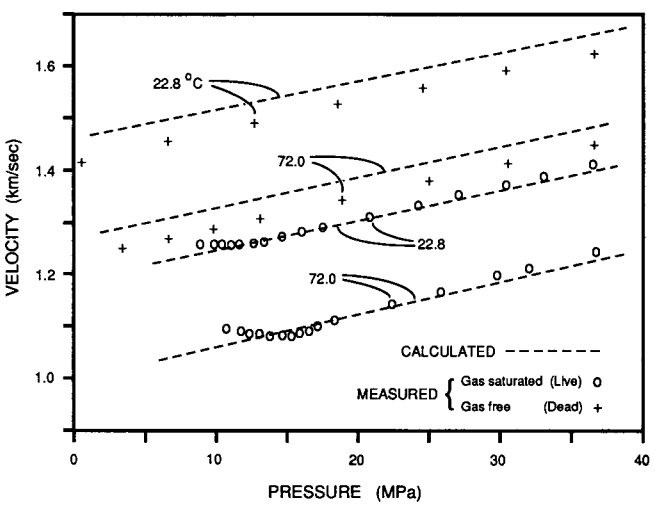

FIG. 8. Acoustic velocity of an oil both with gas in solution (live) and without (dead). Oil reference density, $\rho_0 = 0.916$ (API = 23), gas-oil ratio, R_G, is about 85 L/L. Measurements were made at 22.8 and 72.0°C. As the "bubble point" at 20 MPa is passed with decreasing pressure, free gas begins to come out of solution from the gas charged oil.

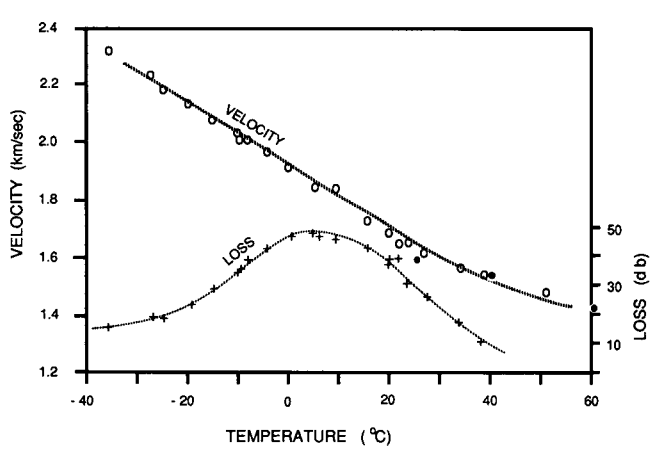

FIG. 9. Velocity and "loss" in a heavy oil as a function of temperature. The loss is just the signal amplitude compared with the amplitude at high temperature and is not corrected for geometric effects, changes in reflection coefficient, etc. Solid circles are the velocity data from Wang (1988) for this oil. The dominant frequency was approximately 800 kHz.

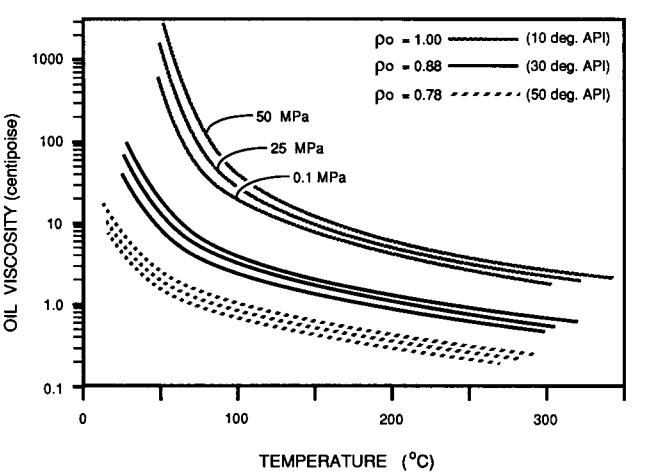

FIG. 10. Oil viscosity as a function of pressure, temperature, and reference density. For gas saturated oils, a pseudodensity is calculated first and then applied to the viscosity relationships. Note that some of the values in this figure are extrapolations beyond the data limits of Beggs and Robinson (1975).

BRINE

The most common pore fluid is brine. Brine compositions can range from almost pure water to saturated saline solutions. Figure 11 shows salt concentrations found in brines from several wells in Arkansas and Louisiana. Gulf of Mexico area brines often have rapid increases in salt concentration. In other areas, such as California, the concentrations are usually lower but can vary drastically among adjacent fields. Brine salinity for an area is one of the easiest variables to ascertain because brine resistivities are routinely calculated during most well log analyses. Simple relationships convert brine resistivity to salinity at a given temperature (e.g., Schlumberger log interpretation charts, 1977). However, local salinity is often perturbed by ground water flow, shale dewatering, or adjacent salt beds and domes.

The thermodynamic properties of aqueous solutions have been studied in detail. Keenen et al., (1969) gives a relation for pure water that can be iteratively solved to give densities at pressure and temperature. Helgeson and Kirkham (1974) used these and other data to calculate a wide variety of properties for pure water over an extensive temperature and pressure range. From their tabulated values of density, thermal expansivity, isothermal compressibility, and constant pressure heat capacity, the heat capacity ratio γ for pure water can be calculated using equation (6). Using this ratio with the tabulated density and compressibility yields the acoustic velocities shown in Figure 12. Water and brines are unusual in having a velocity inversion with increasing temperature.

Increasing salinity increases the density of a brine. Rowe and Chou (1970) presented a polynomial to calculate specific volume and compressibility of various salt solutions at pressure over a limited temperature range. Additional data on sodium chloride solutions were provided by Zarembo and Fedorov (1975), and Potter and Brown (1977). Using these data, a simple polynomial in temperature, pressure, and salinity can be constructed to calculate the density of sodium chloride solutions.

$$\rho_W = 1 + 1 \times 10^{-6}(-80T - 3.3T^2 + 0.00175T^3 + 489P - 2TP + 0.016T^2P - 1.3 \times 10^{-5}T^3P - 0.333P^2 - 0.002TP^2) \quad (27a)$$

and

$$\rho_B = \rho_W + S\{0.668 + 0.44S + 1 \times 10^{-6}[300P - 2400PS + T(80 + 3T - 3300S - 13P + 47PS)]\}, \quad (27b)$$

where ρ_W and ρ_B are the densities of water and brine in g/cm^3, and S is the weight fraction (ppm/1000000) of sodium chloride. The calculated brine densities, along with selected data from Zarembo and Fedorov (1975) are plotted in Figure 13. This relationship is limited to sodium chloride solutions and can be in considerable error when other mineral salts, particularly those producing divalent ions, are present.

A vast amount of acoustic data is available for brines, but generally only under the pressure, temperature, and salinity conditions found in the oceans (e.g., Spiesberger and Metzger, 1991). Wilson (1959) provides a relationship for the velocity V_W of pure water to 100°C and about 100 MPa.

$$V_W = \sum_{i=0}^{4} \sum_{j=0}^{3} w_{ij} T^i P^j, \quad (28)$$

where constants w_{ij} are given in Table 1. Millero et al., (1977) and Chen et al., (1978) gave additional factors to be added to the velocity of water to calculate the effects of

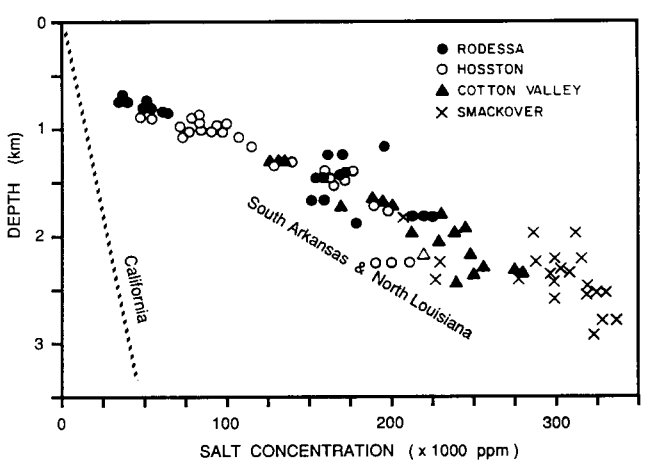

FIG. 11. Salt concentration in sand waters versus depth in southern Arkansas and northern Louisiana (after Price, 1977; and Dickey, 1966). These Gulf Coast data are for basins in which bedded salts are present. The relationship of increasing formation water salinity with increasing depth within the normally pressured zone generally holds for petroleum basins. However, in basins with only clastic sediments and no bedded salts, the maximum salinities will be much less. The California petroleum basins (Ventura, Los Angeles, Sacramento Valley, San Joaquin, etc.) rarely exceed 35 000 ppm salt and the bulk are well below 30 000 ppm.

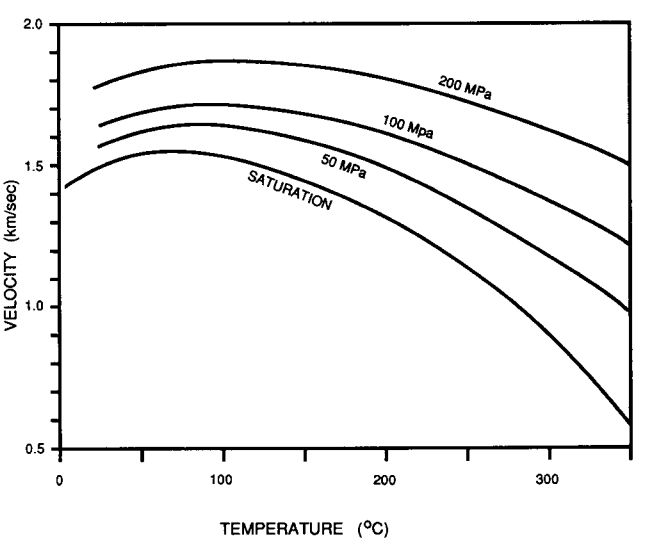

FIG. 12. The sonic velocity of pure water. These values were calculated from the data of Helgeson and Kirkham (1974). "Saturation" is the pressure at which vapor and liquid are in equilibrium.

salinity. Their corrections, unfortunately, are limited to 55°C and 1 molal ionic strength (55 000 ppm). We can extend their results by using the data of Wyllie et al., (1956) to 100°C and 150 000 ppm NaCl. We could find no data in the high temperature, pressure, and salinity region.

As with the gases, since we have an estimate of the heat capacity ratio and the density relation of equation (27) provides us with an equation of state, we could calculate the velocity and modulus at any pressure, temperature, and salinity. However, equation (27) is so imprecise that the calculated values are in considerable disagreement with the low temperature data that exists. A more accurate procedure is to start with the lower temperature and salinity data and use the pure water velocities calculated from Helgeson and Kirkham (1974), and then let the general trend of velocity change indicated by equation (27) provide estimates at higher temperatures and salinities. We can use a simplified form of the velocity function provided by Chen et al., (1978) with the constants modified to fit the additional data.

$$V_B = V_W + S(1170 - 9.6T + 0.055T^2 - 8.5 \times 10^{-5}T^3 + 2.6P - 0.0029TP - 0.0476P^2) + S^{1.5}(780 - 10P + 0.16P^2) - 820S^2. \quad (29)$$

Table 1. Coefficients for water properties computation.

$w_{00} = 1402.85$	$w_{02} = 3.437 \times 10^{-3}$
$w_{10} = 4.871$	$w_{12} = 1.739 \times 10^{-4}$
$w_{20} = -0.04783$	$w_{22} = -2.135 \times 10^{-6}$
$w_{30} = 1.487 \times 10^{-4}$	$w_{32} = -1.455 \times 10^{-8}$
$w_{40} = -2.197 \times 10^{-7}$	$w_{42} = 5.230 \times 10^{-11}$
$w_{01} = 1.524$	$w_{03} = -1.197 \times 10^{-5}$
$w_{11} = -0.0111$	$w_{13} = -1.628 \times 10^{-6}$
$w_{21} = 2.747 \times 10^{-4}$	$w_{23} = 1.237 \times 10^{-8}$
$w_{31} = -6.503 \times 10^{-7}$	$w_{33} = 1.327 \times 10^{-10}$
$w_{41} = 7.987 \times 10^{-10}$	$w_{43} = -4.614 \times 10^{-13}$

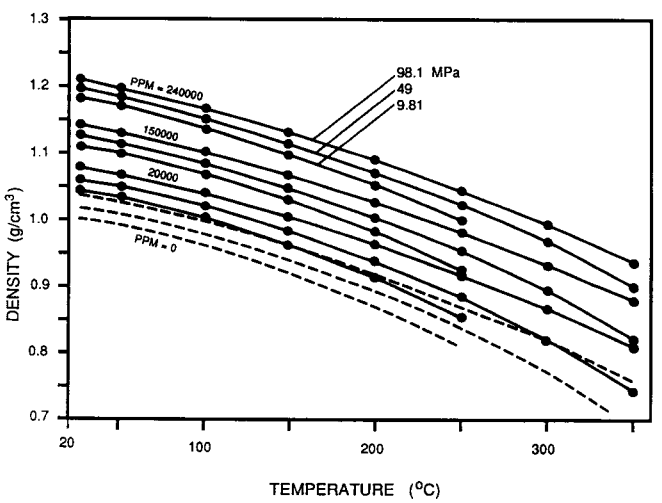

FIG. 13. Brine density as a function of pressure, temperature, and salinity. The solid circles are selected data from Zarembo and Fedorov (1975). The lines are the regression fit to these data. "PPM" refers to the sodium chloride concentration in parts per million.

The calculated moduli using equations (27) and (29) are shown in Figure 14.

Gas can also be dissolved in brine. The amount of gas that can go into solution is substantially less than in light oils. Nevertheless, some deep brines contain enough dissolved gas to be considered an energy resource. Culbertson and McKetta (1951), Sultanov et al., (1972), Eichelberger (1955), and others have shown that the amount of gas that will go into solution increases with pressure and decreases with salinity. For temperatures below about 250°C the maximum amount of methane that can go into solution can be estimated using the expression

$$\mathrm{Log}_{10}(R_G) = \mathrm{Log}_{10}\{0.712P|T - 76.71|^{1.5} + 3676P^{0.64}\} - 4 - 7.786S(T + 17.78)^{-0.306}, \quad (30)$$

where R_G is the gas-water ratio at room pressure and temperature. Dodson and Standing (1945) found that the solution's isothermal modulus K_G decreases almost linearly with gas content.

$$K_G = \frac{K_B}{1 + 0.0494R_G}, \quad (31)$$

where K_B is the bulk modulus of the gas-free brine. Equation (32) shows that for a reasonable gas content, say 10 L/L, the isothermal modulus will be reduced by a third. We presume that the adiabatic modulus, and hence the velocity, will be similarly affected. Substantial decreases in brine velocity upon saturation with a gas were reported by Sergeev (1948).

We conclude this description of brines with a brief look at viscosity. Brine viscosity decreases rapidly with temperature but is little affected by pressure. Salinity increases the viscosity, but this increase is temperature dependent. Matthews and Russel (1967) presented curves for brine viscosity at temperature, pressure, and salinity. Kestin et al., (1981) developed several relationships to describe the viscosity. The results are shown in Figure 15. For temperatures below about 250°C the viscosity can be approximated by

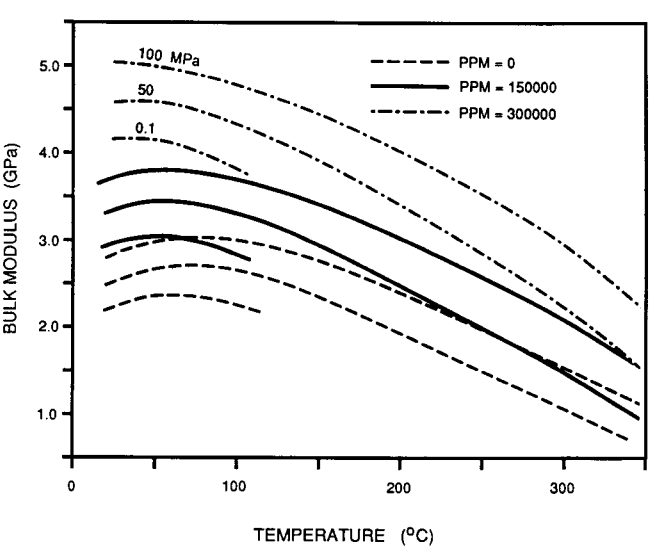

FIG. 14. Calculated brine modulus as a function of pressure, temperature, and salinity.

$$\eta = 0.1 + 0.333S + (1.65 + 91.9S^3) \exp\{-[0.42(S^{0.8} - 0.17)^2 + 0.045]T^{0.8}\}. \quad (32)$$

No pressure effect is considered in this approximation since even at 50 MPa the viscosity is increased only a few percent. Gas in solution lowers brine viscosity; but because much less gas can go into solution than in a light oil, we expect only a small change for live brine viscosity.

FLUID MIXTURES

So far we have dealt only with single phase fluids. Even the gas-saturated (live) fluids near the bubble point were presumed to have no separate gas phase. However, from an exploration standpoint, pore fluid mixtures of liquid and gas phases are extremely important. An oil or gas reservoir above the water contact usually has substantial water trapped in the pore spaces. During production, gas often exsolves from oils due to the pressure drop. The seismic character of such oil reservoirs can change significantly with time. Similar character changes occur during many secondary and tertiary production processes as one fluid mingles with and then displaces another. Hence, for geophysical examinations of reservoirs we must have a way to derive the properties of mixed pore fluid phases.

The density of a mixture is straightforward. Mass balance requires an arithmetic average of the separate fluid phases.

$$\rho_m = \phi_A \rho_A + \phi_B \rho_B. \quad (33)$$

Here, ρ_m is the mixture density, ρ_A and ρ_B, and ϕ_A and ϕ_B, are the densities and volume fractions of components A and B, respectively. The total volume of the mixture, $\bar{V}_M$, is just the sum of the two component volumes $\bar{V}_A$ and $\bar{V}_B$.

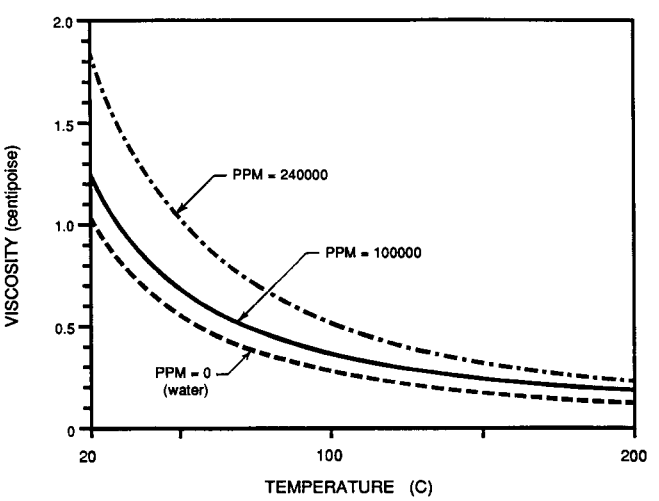

FIG. 15. Brine viscosity as a function of pressure, temperature, and salinity using the relationships of Kestin et al. (1981) are extrapolated using the curves of Matthews and Russel (1967). Above 100°C, the values are at saturation pressure (vapor and liquid are in equilibrium). The pressure dependence is small and not shown for clarity.

The effective modulus of the mixed phase fluid is easily calculable if we assume that the pressures in the two phases are always equal. (We must also assume that there is no mass interchange between the two phases during the passage of a sonic wave; otherwise, the analysis becomes considerably more complex). For any change in pressure, we get a change in each component volume. For example,

$$d\bar{V}_A = (-\bar{V}_A \beta_A \partial P)_S = \left(\frac{\bar{V}_A}{K_A} \partial P\right)_S, \quad (34)$$

where K_A is the adiabatic bulk modulus and β_A is the compressibility of component A. The total volume change for the mixture will be the sum of these changes.

Hence, for a mixture

$$\frac{1}{K_M} = \frac{1}{\bar{V}_A + \bar{V}_B} \frac{1}{\partial P}\left(\frac{\bar{V}_A}{K_A} \partial P + \frac{\bar{V}_B}{K_B} \partial P\right) \quad (35a)$$

$$= \frac{\phi_A}{K_A} + \frac{\phi_B}{K_B}. \quad (35b)$$

This is also known as Wood's equation. Thus, if we know the properties of the individual fluids and their volume fraction, the properties of the mixture can be calculated.

The well-known and dramatic velocity decrease caused by a small amount of free gas phase is explained by equations (33) and (35). For a small amount of gas, the density of the mixture is dominated by the liquid. However, since the modulus of the gas is so small, even a tiny amount will dramatically affect the inverse relationship in equation (35). Figure 16 shows the modulus of a mixture of brine and free gas as a function of composition and pressure. This behavior is responsible for the seismic reflection bright spot effect over gas deposits. The drop in the mixture modulus as small amounts of a gas phase are introduced is less abrupt at higher pressures because of the increased gas modulus. Thus bright spots detected at greater depths require higher gas saturation.

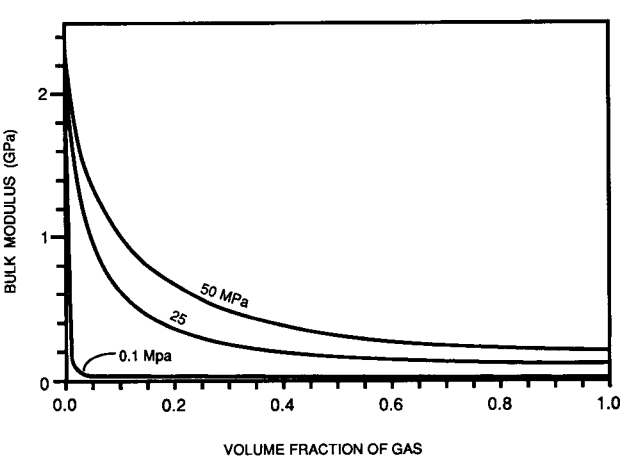

FIG. 16. The calculated bulk modulus for mixtures of gas (G = 0.6) and brine (50 000 ppm NaCl). The approximate in-situ temperatures were used at each pressure (0.1 MPa-20°C; 25 MPa-68°C; 50 MPa-116°C).

The situation is more complex if we examine mixtures of brine and oil. As oil absorbs gas, its properties approach those of the free gas phase. The modulus of a brine-oil mixture is shown in Figure 17 both for constant composition liquids and for gas-saturated liquids at pressure and temperature. Increasing gas content decreases K_{oil} with increasing pressure. If we compare Figures 16 and 17, we see that, with increasing pressure (depth) a gas-saturated (live) oil appears much like a gas. Thus, estimates of in-situ pore fluids can be in substantial error when dissolved gas is not considered. Figure 17 indicates how bright spots can be developed off brine/oil interfaces as observed by Hwang and Lellis (1988) and Clark (1992).

ADDITIONAL CONSIDERATIONS

This analysis of fluid properties has included brines, oils, and gases under pressures and temperatures typically encountered in exploration. By using these properties in such models as those by Gassmann (1951) or Biot (1956a, b and 1962) the effects of different pore fluids on rock properties can be calculated. However, many factors can intervene to alter the fluid and rock properties estimated under the simplistic conditions we have assumed.

Rocks are not the inert and passive skeletons usually assumed in composite media theory. Considerable amounts of fluid/rock interactions occur under natural circumstances. In particular, water layers become bound to the surface of mineral grains. Electrical conductivity measurements and expelled fluid analyses indicate that such bound water will have significantly different properties than those of bulk pore water. This interaction effect will increase in rocks as the grain or pore size get smaller and mineral surface areas increase. Much of the water in a shale may behave more like a gel than like a free-water phase.

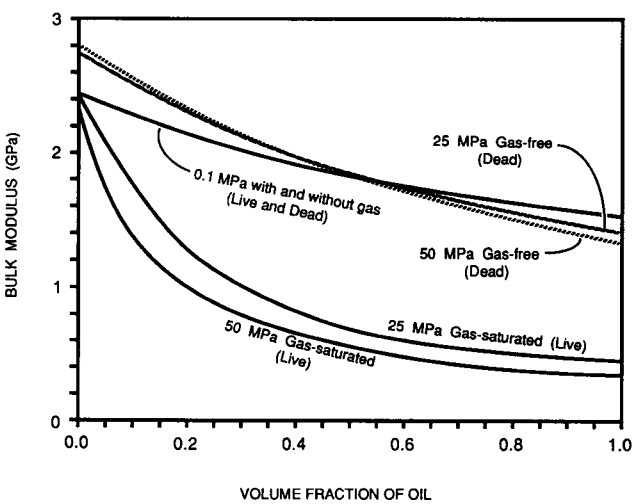

FIG. 17. The calculated modulus of a mixture of light oil (ρ_0 = 0.825, API = 40) and brine (50 000 ppm NaCl). Curves include both "live" mixtures saturated with gas in both oil and brine, and "dead" liquids with no gas in solution. The approximate in-situ temperatures were used at each pressure (0.1 MPa-20°C; 25 MPa-68°C; 50 MPa-116°C).

Further, as pore size decreases in a rock, the boundary conditions of our model change. We had assumed that as a wave passes, heat could not be conducted and so the process was adiabatic (even as the frequency is lowered, the wavelength and distance that heat must travel are proportionately increased). In reality, as a wave passes through a mixture of gas and liquid phases, most of the work is done on the gas phase but most of the heat resides in the liquid. Most of the adiabatic temperature changes are in the gas phase. If the particle size of the mixture is small enough, significant heat can be exchanged between the phases. The process is then isothermal and not adiabatic. This effect would lead to frequency dependent rock properties. In any case, since adiabatic and isothermal properties are usually so close, the results of this effect should be small.

Another factor neglected in our analysis is surface tension. If a fluid develops a surface tension at an interface, then a phase in a bubble within this fluid will have a slightly higher pressure. For a gas bubble within a brine,

$$P_G = P_B + \frac{2\sigma}{r}, \tag{36}$$

where P_G and P_B are the pressures within the gas and brine, respectively, σ is the surface tension, and r is the bubble radius. We see from this equation that as the radius decreases, the pressure inside the bubble could become substantial. As the gas pressure increases, the gas modulus and density increase. At small enough radii, high enough P_G, the gas will condense into a liquid. Kieffer (1977) examined this effect for air-water mixtures to evaluate its possible influence on the mechanics of erupting volcanoes and geysers. Her calculations indicated that the effect will become pronounced when the bubble radii go below about 100 angstroms. This is the pore size (and therefore bubble size) found in shales and fine siltstones (Hinch, 1980). To the extent that this equation remains valid at such small radii, the depression of rock velocity expected from partial gas saturation, as was indicated in Figure 16, will be precluded from shales. This important topic requires further investigation.

Last, in natural systems, the behavior of the fluids can be much more complex than we have described. Other compounds are often present, either as components of the gases, oils, or brines, or as separate phases. For example, under certain pressures and temperatures, hydrocarbon gases will react with water to form hydrates. The hydrocarbons themselves are usually complex chemical systems with pseudo-critical points, retrograde condensation, phase compositional interaction, and other behaviors that can only be described with a far more detailed analysis than we have provided. These subtleties can become important, particularly in reservoir geophysics where fluid identification and phase boundary location are primary concerns.

CONCLUSIONS

The primary seismic properties of pore fluids: density, bulk modulus, velocity, and viscosity, vary substantially but systematically under the pressure and temperature conditions typical of oil exploration. Brines and hydrocarbon gases and oils are the most abundant pore fluids and their

properties are usually oversimplified in geophysics. In particular, light oils can absorb large quantities of gas at elevated pressures significantly reducing their modulus and density. This reduction can be sufficient to cause reflection bright spots of oil-brine contacts. With simple estimates of composition and the in-situ pressure and temperature, more realistic properties can be calculated.

ACKNOWLEDGMENTS

We wish to express our thanks to the ARCO Oil and Gas Company for encouraging this research. John Castagna, Jamie Robertson, Robert Withers, and Vaughn Ball gave many helpful comments on the manuscript. Matt Greenberg contributed useful references and ideas. Bill Dillon, Anthony Gangi and others provided very constructive reviews leading to substantial improvements in the text. Professor Amos Nur provided valuable support and guidance to Z. Wang on these topics at Stanford University. We also wish to thank Atlantic Richfield Corporation and Core Laboratories Canada for permission to publish this work.

REFERENCES

Beal, C., 1946, The viscosity of air, water, natural gas, crude oil, and its associated gases at oil field temperatures and pressures: Petroleum Trans., Soc. of Petr. Eng. of AIME, **165**, 95–118.

Biot, M. A., 1956a, Theory of propagation of elastic waves in a fluid-saturated porous solid. I. Low-frequency range: J. Acoust. Soc. Am., **28**, 168–178.

——— 1956b, Theory of propagation of elastic waves in a fluid-saturated porous solid. II. Higher frequency range: J. Acoust. Soc. Am., **28**, 179–191.

——— 1962, Mechanics of deformation and acoustic propagation in porous media: J. Appl. Phys., **33**, 1482–1498.

Beggs, H. D., and Robinson, J. R., 1975, Estimating the viscosity of crude oil systems: J. Petr. Tech., **27**, 1140–1141.

Carr, N. L., Kobayashi, R., and Burrows, D. B., 1954, Viscosity of hydrocarbon gases under pressure: Petroleum Trans., Soc. of Petr. Eng. of AIME, **201**, 264–272.

Clark, V. A., 1992, The properties of oil under in-situ conditions and its effect on the seismic properties of rocks: Geophysics, **57**, 894–901.

Castellan, G. W., 1971, Physical chemistry, 2nd Ed.: Addison-Wesley Publ. Co.

Chen, C. T., Chen, L. S., and Millero, F. J., 1978, Speed of sound in NaCl, $MgCl_2$, Na_2SO_4, and $MgSO_4$ aqueous solutions as functions of concentration, temperature, and pressure: J. Acoust. Soc. Am., **63**, 1795–1800.

Culbertson, O. L., and McKetta, J. J., 1951, The solubility of methane in water at pressure to 10,000 PSIA: Petroleum Trans., AIME, **192**, 223–226.

Dickey, P. A., 1966, Patterns of chemical composition in deep subsurface waters: AAPG Bull., **56**, 1530–1533.

Dodson, C. R., and Standing, M. B., 1945, Pressure-volume-temperature and solubility relations for natural-gas-water mixtures: in Drilling and production practices, 1944, Am. Petr. Inst.

Eichelberger, W., 1955, Solubility of air in brine at high pressures: Ind. Eng. Chem., **47**, 2223–2228.

Gammon, B. E., and Douslin, D. R., 1976, The velocity of sound and heat capacity in methane from near-critical to subcritical conditions and equation-of-state implications: J. Chem. Phys., **64**, 203–218.

Gassmann, F., 1951, Elastic waves through a packing of spheres: Geophysics, **16**, 673–685.

Hedberg, H. D., 1974, Relation of methane generation to undercompacted shales, shale diapirs, and mud volcanoes: AAPG Bull., **58**, 661–673.

Helgeson, H. C., and Kirkham, D. H., 1974, Theoretical prediction of the thermodynamic behavior of aqueous electrolytes: Am. J. Sci., **274**, 1089–1198.

Hinch, H. H., 1980, The nature of shales and the dynamics of hydrocarbon expulsion in the Gulf Coast Tertiary section, *in* Roberts, W. H. III, and Cordell, R. J., Eds, Problems of petroleum migration, AAPG studies in geology no. 10: Am. Assn. Petr. Geol., 1–18.

Hwang, L-F., and Lellis, P. J., 1988, Bright spots related to high GOR oil reservoir in Green Canyon: 58th Ann. Internat. Mtg., Soc. Expl. Geophys. Expanded Abstracts, 761–763.

Johnson, R. C., 1972, Tables of critical flow functions and thermodynamic properties for methane and computational procedures for methane and natural gas: NASA SP-3074, National Aeronautics and Space Admin.

Jones, T. D., 1986, Pore fluids and frequency-dependent wave propagation in rocks: Geophysics, **51**, 1939–1953.

Katz, D. L., Cornell, D., Vary, J. A., Kobayashi, R., Elenbaas, J. R., Poettmann, F. H., and Weinaug, C. F., 1959, Handbook of natural gas engineering: McGraw-Hill Book Co.

Keenen, J. H., Keyes, F. G., Hill, P. G., and Moore, J. G., 1969, Steam tables: John Wiley & Sons, Inc.

Kestin, J., Khalifa, H. E., and Correia, R. J., 1981, Tables of the dynamic and kinematic viscosity of aqueous NaCl solutions in the temperature range 20–150°C and the pressure range 0.1–35 MPa: J. Phys. Chem. Ref. Data, **10**, 71–74.

Kieffer, S. W., 1977, Sound speed in liquid-gas mixtures: Water-air and water-steam: J. Geophys. Res., **82**, 2895–2904.

Kuster, G. T., and Toksöz, M. N., 1974, Velocity and attenuation of seismic waves in two-phase media: Part 1. Theoretical formulations: Geophysics, **39**, 587–606.

McCain, W. D., 1973, Properties of petroleum fluids: Petroleum Pub. Co.

Millero, F. J., Ward, G. K., and Chetirkin, P. V., 1977, Relative sound velocities of sea salts at 25°C: J. Acoust. Soc. Am., **61**, 1492–1498.

Matthews, C. S., and Russel, D. G., 1967, Pressure buildup and flow tests in wells, Monogram Vol. 1, H. L. Doherty Series: Soc. Petr. Eng. of AIME.

Mavko, G. M., and Jizba, D., 1991, Estimating grain-scale fluid effects on velocity dispersion in rocks: Geophysics, **56**, 1940–1949.

Nur, A., and Simmons, G., 1969, The effect of viscosity of a fluid phase on the velocity in low porosity rocks: Earth Plan. Sci. Lett., **7**, 99–108.

O'Connell, R. J., and Budiansky, B., 1974, Seismic velocities in dry and saturated cracked solids: J. Geophys. Res., **79**, 5412–5426.

——— 1977, Viscoelastic properties of fluid-saturated cracked solids: J. Geophys. Res., **82**, 5719–5735.

Potter, R. W., II, and Brown, D. L., 1977, The volumeteric properties of sodium chloride solutions from 0 to 500 C at pressures up to 2000 bars based on a regression of available data in the literature: U.S. Geol. Surv. Bull 1421-C.

Price, L. C., 1977, Geochemistry of geopressured geothermal waters from the Texas Gulf coast: *in* J. Meriwether, Ed., Proc. Third Geopressured-geothermal Energy Conf., **1**, Univ. S. Louisiana.

Rao, K. S., and Rao, B. R., 1959, Study of temperature variation of ultrasonic velocities in some organic liquids by modified fixed-path interferometer method: J. Acoust. Soc. Am., **31**, 439–431.

Rowe, A. M., and Chou, J. C. S., 1970, Pressure-volume-temperature-concentration relation of aqueous NaCl solutions: J. Chem. Eng. Data, **15**, 61–66.

Schlumberger, Inc., 1977, Log interpretation charts: Schlumberger, Inc.

Sergeev, L. A., 1948, Ultrasonic velocities in methane saturated oils and water for estimating sound reflectivity of an oil layer, Fourth All-Union Acoust. Conf. Izd. Nauk USSR. (English trans).

Sokolov, V. A., 1968, Theoretical basis for the formation and migration of oil and gas: *in* Origin of petroleum and gas, Nauka, Moscow, (English trans), 4–24.

Spiesberger, J. L., and Metzger, K., 1991, New estimates of sound speed in water: J. Acoust. Soc. Am., **89**, 1697–1700.

Standing, M. B., 1962, Oil systems correlations, *in* Frick, T. C., Ed., Petroleum production handbook, volume II: McGraw-Hill Book Co., part 19.

Sultanov, R. G., Skripka, V. G., and Namiot, A. Y., 1972, Solubility of methane in water at high temperatures and pressures: Gazovaia Prommyshlenmost, **17**, 6–7, (English trans).

Thomas, L. K., Hankinson, R. W., and Phillips, K. A., 1970, Determination of acoustic velocities for natural gas: J. Petr. Tech., **22**, 889–892.

Tittmann, B. R., Bulau, J. R., and Abdel-Gawad, M., 1984, The role of viscous fluids in the attenuation and velocity of elastic waves in porous rocks, *in* Johnston, D. L., and Sen, P. S., Eds., Physics and chemistry of porous materials: AIP Conf. Proc., **107**, 131–143.

Vo-Thanh, D., 1990, Effects of fluid viscosity on shear-wave attenuation in saturated sandstones: Geophysics, **55**, 712–722.

Wang, Z-W., 1988, Wave velocities in hydrocarbons and hydrocarbon saturated rocks—with applications to EOR monitoring: Ph.D. thesis, Stanford Univ.

Wang, Z., Batzle, M. L., and Nur, A., 1990, Effect of different pore fluids on seismic velocities in rocks: Can. J. Expl. Geophys., **26**, 104–112.

Wang, Z., and Nur, A., 1986, The effect of temperature on the seismic wave velocities in rocks saturated with hydrocarbons: Soc. Petr. Eng. (SPE) paper 15646, Proc. 61st Soc. Petr. Eng. Tech. Conf.

Wang, Z., Nur, A., and Batzle, M. L., 1988, Acoustic velocities in petroleum oils: Soc. Petr. Eng. (SPE) paper 18163, Proc. 63rd Soc. Petr. Eng. Tech. Conf., Formation Eval. Res. Geol. Section, 571–585.

Wilson, W. D., 1959, Speed of sound in distilled water as a function of temperature and pressure: J. Acoust. Soc. Am., **31**, 1067–1072.

Wyllie, M. R. J., Gregory, A. R., and Gardner, L. W., 1956, Elastic wave velocities in heterogenious and porous media: Geophysics, **21**, 41–70.

Younglove, B. A., and Ely, J. F., 1987, Thermophysical properties of fluids. II. Methane, ethane, propane, isobutane, and normal butane: J. Phys. Chem. Ref. Data, **16**, 557–797.

Zarembo, V. I., and Fedorov, M. K., 1975, Density of sodium chloride solutions in the temperature range 25–350°C at pressures up to 1000 kg/cm^2: J. Appl. Chem. USSR, **48**, 1949–1953, (English trans).